J. Mater. Environ. Sci. 6 (11) (2015) 3094-3109
ISSN : 2028-2508
CODEN: JMESCN

Structural study and vibrational analyses of the monomeric, dimeric, trimeric and tetrameric species of acetamide by using the FT-IR and Raman spectra, DFT calculations and SQM methodology

H. Abdelmoulahi[1], H. Ghalla[2,*], S. A. Brandán[3], S. Nasr[1]

[1]*University of Monastir, Laboratory of Physical-Chemistry of Materials, Faculty of Science, Monastir 5079, Tunisia.*
[2]*University of Monastir, Quantum Physics Laboratory, Faculty of Science, Monastir 5079, Tunisia.*
[3]*Cátedra de Química General, Facultad de Bioquímica, Química y Farmacia, Universidad Nacional de Tucumán, Ayacucho 471, T 4000 CAN, San Miguel de Tucumán, Tucumán, R. Argentina.*

Received 17 Mar 2015, Revised 19 Aug 2015, Accepted 21 Aug 2015
[*]*Corresponding Author. E-mail: houcineghalla@yahoo.fr*

Abstract
Structural and vibrational study of acetamide and its hydrogen bonded dimer, trimer and tetramers have been performed using DFT/B3LYP method with 6-311++G(d,p) basis set. Particular attention has been focused on the intermolecular N-H···O hydrogen bonding forming the acetamide species. Natural Bond Orbital (NBO) analysis is performed in order to explore interactions and charge transfer among different orbitals and lone pairs taking place within the acetamide species. In addition, the Atomic in Molecule (AIM) analysis is used to study the properties of the intermolecular hydrogen bonding in the acetamide complexes on the basis of topological parameters calculated at bond critical points. The DFT calculations were combined with Pulay's scaled quantum mechanics force field (SQMFF) methodology to fit the calculated wavenumbers to the experimental ones. Moreover, the red shifts of N-H and C=O stretching vibrational modes upon formation of the hydrogen bonded acetamide species have been discussed.

Keywords: DFT calculations, acetamide species, hydrogen bond, NBO and AIM analysis, vibrational spectra.

1. Introduction
Hydrogen bonds are crucial to understanding many biochemical activities and biological processes [1-5]. These interactions have been widely investigated by numerous experimental and theoretical studies [6-12]. Acetamide and some of its derivatives are capable of forming N-H···O and C-H···O hydrogen bonds. In this context, a DFT study of hydrogen bond properties of peptide group in crystalline structure of acetamide [13] has been reported by Samadi et al. Further, Esrafili et al. [14] have systematically examined the properties of N-H···O interactions in various linear acetamide clusters based on MP2 and DFT methods. They have discussed the structures, binding energies, vibrational frequencies, 14N quadrupole coupling properties, hydrogen bonding cooperativity and its dependence on cluster size. Based on the NBO and topological AIM analyses, the authors have showed that the delocalization energy of LP(O)→σ*(N-H) interaction increases with the number of acetamide molecules in the cluster and that also the capacity of the acetamide clusters to concentrate electrons at the hydrogen bond critical points increases with the size of the cluster.
In the same spirit, Mahadevi et al. [15] have reported a theoretical study of linear, circular and standard arrangements of acetamide clusters. They have showed a clear manifestation of cooperativity in hydrogen bonding in all the cluster forms as evidenced by the corresponding increase in interaction energy per monomer with an increase in the cluster size. Recently, using the HF and DFT methods, Beg et al. have investigated the double proton transfer mechanism in the acetamide dimer in terms of the energy profile, reaction force, chemical

hardness, average polarizability, ionization potential, chemical potential and interaction energies [16].
Recently, we have discussed the intermolecular association in liquid acetamide at 346 K by using X-ray diffraction data in combination with MP2 optimized geometries of some acetamide clusters [17]. Different models including dimer, trimer and tetramer have been proposed to describe the intermolecular hydrogen bonds in the local order of the liquid acetamide. By comparing the theoretical and experimental data, it has been found that the dimer and tetramer structures can be considered a probable species to describe the intermolecular arrangement of the acetamide structure in the liquid but, in that work the vibrational analysis was not considered.
Hence, in this work we have focused the intermolecular interactions in the acetamide clusters from both structural and vibrational points of view by combining the DFT calculations and the SQM methodology in order to have a complete insight of the nature of those interactions. The structural parameters and vibrational frequencies of acetamide monomer and its hydrogen bonded dimer, trimer and tetramers are carried out using the B3LYP/6-311++G** level of theory. The properties of the intermolecular N-H···O and C-H···O hydrogen bonds and the topological properties are discussed on the basis of NBO [18-21] and AIM [20-23] analyses. The vibrational assignments of the observed bands to the vibration normal modes for all acetamide species are performed using Pulay's Scaled Quantum Mechanics Force Field (SQMFF) methodology [24].

2. Experimental

The title compound was purchased from Sigma-Aldrich Chemical Company (USA). FT-IR spectrum of acetamide was recorded in the region 4000-400 cm^{-1} on JASCO-6300 spectrometer with samples in the KBr. The FT-Raman spectrum of the molecule was obtained in the range 4000-100 cm^{-1} using Bruker RFS 100/s FT-Raman spectrophotometer with a 1064 nm Nd:Yag laser source of 150 mW power. The spectral resolution is 2 cm^{-1}.

3. Computational Details

The monomeric, dimeric, cyclic trimeric and two tetrameric species were firstly modeled with GaussView program [25] taking into account the experimental crystalline structure of acetamide determined by X-ray diffraction [26]. Then, all those species were optimized at B3LYP/6-311++G** level of theory by using the Gaussian 09 program [27]. The interaction energies for the acetamide dimer, trimer and tetramers were considered as the difference between the total energy of the complex and the separate monomers. Additionally, the Boys-Bernardi counterpoise correction method [28] was applied to find the basis set superposition error (BSSE) corrected interaction energies. The intermolecular interactions and their corresponding stabilization energies were obtained by means of NBO calculations using the NBO 3.1 program [19], as implemented in the Gaussian 09 program [27]. The topological analysis of the hydrogen bonds interactions formed in the different acetamide species have been performed using AIM2000 software program [29] to get a deeper insight of the nature of these interactions. The B3LYP/6-311++G** method was also used to calculate the harmonic wavenumbers and the corresponding valence force fields, expressed in cartesian coordinates. The natural internal coordinates for all the species of acetamide were defined according to those reported for similar molecules [30-36]. The resulting force fields in cartesian coordinates for all the species of acetamide were transformed to "natural" internal coordinates employing the MOLVIB program [37]. The complete assignment was then performed, taking into account the resulting SQM. The nature of all of the normal modes of vibration was verified by GaussView program.

4. Results and Discussion

4.1. Geometry optimization

The initial structures of acetamide monomer, dimer, trimer and tetramers were optimized at B3LYP/6-311++G** level of theory and, in all them no imaginary frequencies were found. Besides, each of them corresponds to a minimum on the potential surface. The optimized molecular structures along with numbering of atoms of monomer, dimer, trimer, tetramer 1 and tetramer 2 of acetamide are shown in Figure 1. In tetramer 1, four

acetamide molecules are held together by two N-O···H and two C-O···H hydrogen bonds, whereas the tetramer 2 exhibits only N-O···H type of interaction. The optimized geometrical parameters together with the Root Mean Square Deviation (RMSD) of all the acetamide species are listed and compared to the experimental values [26] in Tables 1 and 2. The X-ray data showed that the acetamide molecules in the crystalline structure are held together by N-O···H intermolecular hydrogen bonds varied from 2.011 to 2.092 Å [26]. In relation to the monomer, the calculations show that the acetamide monomer has a planar C_s symmetry group. The comparison between the calculated geometrical parameters and the X-ray data reveals that the calculated N-H bond lengths (1.008 and 1.005 Å) are larger than the experimental values (0.898 and 0.870 Å). The calculated C=O bond length (1.217 Å) is relatively shorter than the experimental value (1.241 Å). For the C-N bond length, the calculated value is about 1.367 Å, which is considerably larger than the X-ray one (1.325 Å). Further, the calculated O-C-N angle is found to be 122°, which is slightly larger than that measured in the crystalline form (121.8°). The difference between the calculated and experimental data may be explained principally by the presence of intermolecular hydrogen bonding between acetamide molecules.

Upon dimerization, the geometry of the acetamide monomer has been considerably changed. The dimeric form exhibits a cyclic C_i symmetry group with two identical N-H···O hydrogen bonds. The formation of the dimer induces a small elongation of the N-H and C-O bond lengths involved in the hydrogen bonds. Moreover, the calculated O2···H14 and O11···H4 intermolecular hydrogen bonds are found to be 1.868 Å. These bond lengths are considerably smaller than that found in the crystalline structure (2.027 and 2.051 Å).

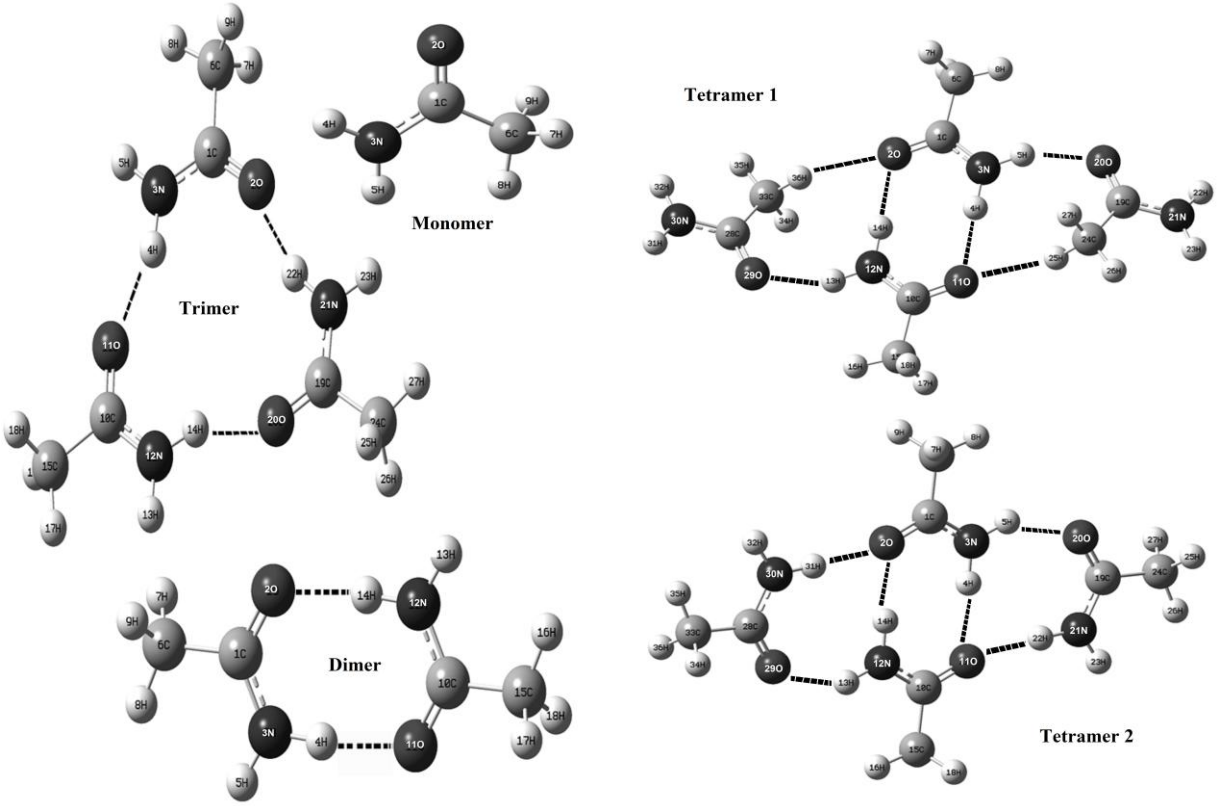

Figure 1: Optimized geometrical structures of acetamide monomer, dimer, trimer, tetramer 1 and tetramer 2 along with number of atoms calculated by using B3LYP/6-311++G** level. The hydrogen bonding is indicated by dashed lines.

The acetamide trimer has a planar cyclic structure with C_{3h} symmetry group. The three acetamide molecules are connected by three closely identical hydrogen bonds O11···H4, O2···H22 and O20···H14 which are equal to 1.878, 1.879 and 1.880 Å, respectively. So, all hydrogen bond distances involved in the trimer structure are longer than those found in the dimer one. This fact can be explained by the larger internuclear distances in the acetamide trimer leading to weaker intermolecular interactions in comparison with the corresponding interactions

in the dimer structure. The calculation showed also that the formation of the acetamide trimer leads to a decrease reaching 17° of the N-H···O hydrogen bonded angles in comparison with the dimer. Accordingly, we may conclude that the hydrogen bonds in the trimer are weaker than those formed in the dimer species. The calculations were also carried out for two hydrogen bonded tetramer forms.

Table 1: Geometrical parameters for all the species of acetamide calculated at B3LYP/6-311++G** level along with the experimental values.

Parameter	Monomer	Dimer	Trimer	Tetramer 1	Tetramer 2	Exp. [26]
Bond length (Å)						
C1=O2	1.217	1.233	1.232	1.240	1.245	1.241
C1-N3	1.367	1.348	1.346	1.340	1.334	1.325
C1-C6	1.518	1.516	1.519	1.516	1.513	1.503
RMSD	0.017	0.009	0.009	0.007	0.790	
Bond Angle (º)						
O2-C1-N3	122.0	122.6	123.2	122.8	122.2	121.8
O2-C1-C6	122.1	120.3	120.1	120.2	120.2	120.9
N3-C1-C6	115.8	117.0	116.6	116.9	117.4	117.2
RMSD	0.6	0.3	0.6	0.4	0.3	
Dihedral Angle (º)						
O2-C1-C6-H8	179.9	179.5	179.9	-179.4	179.8	174.9
O2-C1-N3-H5	-179.9	179.9	-179.9	179.5	179.9	173.4
RMSD	176.7	3.9	176.7	177.1	4.1	

Table 2: Hydrogen bonding parameters for the acetamide dimer, trimer, tetramer 1 and tetramer 2 calculated at B3LYP/6-311++G** level along with the experimental values.

	Dimer		Trimer		Tet 1	Tet 2	Exp. [26]
Bond length (Å)							
O2···H14	1.868	O11···H4	1.878	O2···H14	1.910	1.921	2.027
O11···H4	1.868	O20···H14	1.880	O11···H4	1.910	1.921	2.051
		O2···H22	1.879	O2···H36(H31)	2.492	1.969	
				O11···H25(H22)	2.492	1.969	
				O20···H5	2.008	2.046	2.011
				O29···H13	2.008	2.046	2.092
Bond angle (°)							
C1-O2···H14	123.6	C1-O2···H22	151.2	C1-O2···H36	169.0	165.8	120.6
C10-O11···H4	123.6	C10-O11···H4	151.2	C1-O2···H14	116.8	114.4	120.7
		C19-O20···H14	150.7	C10-O11···H4	116.8	114.4	
				C10-O11···H25	169.0	165.8	
				C19-O20···H5	122.9	136.8	
				C28-O29···H13	122.9	136.8	
Dihedral angle (°)							
C1-O2···H14-N	0.4	C1-O2···H22-N	178.1	C1-O2···H36-C(N)	71.1	-1.4	77.9
C10-O11···H4-N	-0.4	C10-O11···H4-N	178.8	C1-O2···H14-N	-138.6	-179.3	-77.9
		C19-O20···H14-N	177.8	C10-O11···H4-N	138.6	-178.4	
				C10-O11···H25-C(N)	-71.1	-0.1	
				C19-O20···H5-N	-14.1	0.0	-57.7
				C28-O29···H13-N	14.1	-0.0	57.7

In the tetramer 1, two acetamide molecules are connected to the dimer through N-H···O and C-H···O hydrogen bonds, while in the tetramer 2, all the acetamide molecules are connected by N-H···O hydrogen bond type. It has been observed that the formation of tetramer species produced a noticeable lengthening of the hydrogen bonds, in comparison to the dimer structure. As shown in Table 2, the hydrogen bond lengths are increased from 1.868 Å in the dimer to 1.910 and 1.921Å in tetramer 1 and tetramer 2, respectively. In the tetramer 1, the new formed hydrogen bond lengths between the CH_3 groups and O2 and O11 atoms are found to be 2.492 Å, while the N-H···O hydrogen bonds are about 2.008 Å. In the tetramer 2, the acetamide molecules are associated to the dimer structure through N-H···O hydrogen bonds of about 1.970 and 2.047 Å.
According to the above calculated geometrical structures, one may conclude that the tetramer 2 reproduces more accurately the experimental values than the other acetamide species. The interaction energies have been computed as the difference between the total energy of the optimized acetamide complex and the sum of the total energies of the optimized isolated monomers at B3LYP/6-311++G** level of theory. In Table 3, we have reported the total energies, zero-point energies, corrected interaction energies, dipole moments and other thermodynamic parameters. Taking into account the ZPVE and BSSE counterpoise corrections, the computed interaction energies are -45.86, -72.93, -87.94 and -114.16 kJ/mol for the dimer, trimer, tetramer 1 and tetramer 2, respectively. Therefore, the interaction energies are consistently improved as the size complex is increased and the tetramer 2 may be considered as the most stable acetamide species.

Table 3: Thermodynamic parameters (at 298.15 K) of acetamide monomer, dimer, trimer, tetramer 1 and tetramer 2 calculated at B3LYP/6-311++G** level.

	Monomer	Dimer	Trimer	Tetramer 1	Tetramer 2
SCF energy (a.u.)	-209.2887	-418.5988	-627.8999	-837.1973	-837.2084
ZPVE (kJ/mol)	191.79	391.96	588.35	786.13	788.52
ΔE (kJ/mol)		-56.23	-89.03	-111.59	-140.71
ΔE^{ZPE} (kJ/mol)		-47.82	-76.06	-92.55	-119.33
BSSE energy (kJ/mol)		1.94	3.15	4.61	5.16
$\Delta E^{ZPE+BSSE}$ (kJ/mol)		-45.86	-72.93	-87.94	-114.16
E_{HB} (kJ/mol)		-22.93	-24.31	-21.97	-28.53
Thermal energy (kJ/mol)	205.69	421.21	636.03	850.99	852.24
Heat capacity (J/mol.K)	68.99	151.81	241.38	330.45	325.60
Entropy (J/mol.K)	307.42	449.11	625.64	779.15	767.49
Dipole moment (Debye)	3.972	0.0021	0.0090	0.0004	0.0117

4.2. NBO analysis
NBO analysis has been performed on the acetamide species in order to understand the hydrogen bonds, intermolecular charge transfer and cooperative effect due to delocalization of electron density from the filled lone pairs LP(O) into the unfilled antibond σ*(N-H) causing stabilization of the hydrogen bonded systems. The stabilization energy $E^{(2)}$ associated with the delocalization between donor (i) and acceptor (j) is estimated from the second-order perturbation approach [38] as given below:

$$E^{(2)} = q_i \frac{F^2(i,j)}{\varepsilon_i - \varepsilon_j} \quad (1)$$

Here q_i is the orbital occupancy, ε_i and ε_j are the diagonal elements and F(i,j) is the off-diagonal NBO Fock matrix element. The larger value of $E^{(2)}$, the more intensive the interaction between electron donors and electron acceptors is, i.e. more donating tendency from electron donors to electron acceptors and greater extent of conjugation of the whole system. The results of second order perturbation theory analysis of Fock matrix for the different acetamide species are collected in Table 4.
In the acetamide monomer, the LP(2)O2→σ*(C1-N3) and LP(1)N3→π*(C1-O2) interactions have an enormous stabilization energies of 104.5 and 239.64 kJ/mol. In the acetamide dimer, the high delocalization energies are

286.29 and 298.45 kJ/mol which are observed for π(N3-H5)→σ*(C1-C2) and π(N12-H13)→σ*(C10-C11) interactions, respectively. In addition the transfer of electron density from the lone pairs LP(2)O2 and LP(2)O11 to the antibonding orbitals σ*N12-H14 and σ*N3-H4 reveals a stabilization energies of about 43.43 kJ/mol.

Table 4: Main delocalization energy (in kJ/mol) for the studied species of acetamide at B3LYP/6-311++G** level of theory.

Delocalization	Monomer	Dimer	Trimer	Tetramer 1	Tetramer 2
π (N3-H5)→σ*(C1-O2)		286.29			
π (N12-H13)→σ*(C10-O11)		298.45			
LP(2)O2→σ*(C1-N3)	104.50	77.08	81.22	72.52	70.43
LP(2)O2→σ*(C1-C6)	80.05	79.21	79.29	77.16	72.86
LP(1)N3→π*(C1-O2)	239.64				
LP(2)O2→σ*(N12-H14)		43.43		42.51	40.88
LP(2)O11→σ*(N3-H4)		43.43	18.77	42.51	40.88
LP(2)O11→σ*(C10-N12)		77.08	81.30	0	0
LP(2)O11→σ*(C10-C15)		79.21	79.34	77.16	72.86
LP (1)O2→σ*(N21-H22)			26.92		
LP (2)O2→σ*(N21-H22)			18.98		
LP (1)N3→σ*(C1-O2)			305.35	266.06	350.33
LP(1)O11→σ*(N3-H4)			26.88		11.87
LP(1)N12→σ*(C10-O11)			305.64	265.72	350.37
LP(2)O20→σ*(C19-N21)			81.26	101.78	89.37
LP(2)O20→σ*(C19-C24)			79.29	67.93	79.17
LP(1)O20→σ*(N12-H14)			26.88		
LP(2)O20→σ*(N12-H14)			18.89		
LP(1)N21→σ*(C19-O20)			303.84		
LP (1)O2→σ*(C33-H36)				3.55	
LP(1)O11→σ*(C10-N12)				72.52	
LP(1)O11→σ*(C24-C25)				3.55	
LP(2)O20→σ*(N3-H5)				16.55	9.74
LP(1)N21→σ*(C19-O20)				172.43	284.78
LP(2)O29→σ*(C28-N30)				101.78	89.37
LP(2)O29→σ*(C28-C33)				67.93	79.17
LP(2)O29→σ*(N12-H13)				16.55	9.74
LP(1)N30→σ*(C28-O29)				172.43	284.83
LP(1)O2→σ* (N30-H31)					27.04
LP(2)O2→σ*(N30-H31)					0.50
LP(1)O2→σ*(N12-H14)					11.87
LP(2)O11→σ*(C10-C15)					70.43
LP(1)O11→σ*(N21-H22)					27.04
LP(2)O11→σ*(N21-H22)					0.50
LP(1)O20→σ*(N3-H5)					12.12
LP(1)O29→σ*(N12-H13)					12.12
$\Delta ET_{LP\rightarrow\sigma^*}$	424.19	984.18	1533.85	1640.65	2098.28

Moreover, other important stabilization energies are identified for the LP(2)O2→σ*C1-C6, LP(2)O11→σ*C10-C15, LP(2)O2→σ*C1-N3 and LP(2)O11→σ*C10-N12 interactions. In the trimer species, the delocalization energy corresponding to the LP(2)O11→σ* (N3-H4) interaction is considerably low as compared with that found

in the dimer while, a contrary relation is observed for the LP(1)O11→ σ*(N3-H4) delocalization, as compared with the tetramer 2. The important interactions observed in the acetamide trimer are from LP(1)N3, LP(1)N12 and LP(1)N21 to σ*(C1-O2), σ*(C10-O11) and σ*(C19-O20) with stabilization energy 305.35, 305.64 and 303.84 kJ/mol, respectively. In the acetamide tetramers, the higher stabilization energies are given to the LP (1)N3→ σ*(C1-O2), LP(1)N12→ σ* (C10-O11) and LP(1)N21→σ*(C19-O20). As can be seen in Table 4, the stabilization energies of these interactions are more significant in the tetramer 2 than the tetramer 1. Moreover, the calculation of total delocalization energy $\Delta ET_{LP\rightarrow\sigma^*}$ arising from interactions between lone pairs of the O and N atoms and the σ* antibonding orbitals reveals a high stability for tetramer 2 ($\Delta ET_{LP\rightarrow\sigma^*}$= 2098.28 kJ/mol) than the tetramer 1 ($\Delta ET_{LP\rightarrow\sigma^*}$= 1640.65 kJ/mol).

4.2. AIM analysis

One of the most useful tools to characterise atomic and molecular interactions, particularly hydrogen bonding, is the topological analysis using 'Atom in molecules' (AIM) theory. The theory of AIM efficiently describes hydrogen bonding and its concept without border. One of the advantages of the AIM theory is that one can obtain information on changes in the electron density distribution as result of either bond formation or complexes formation. According to AIM theory, any chemical bond including hydrogen bonding is characterized by the existence of bond critical point (BCP). After the BCPs have been localized, several properties can be calculated at their position in space. Amongst these, the charge density ρ_{BCP} and the Laplacian of the charge density $\nabla^2\rho_{BCP}$ at BCP are of chief importance. According to Koch and Popelier criteria [39] based on AIM theory, (i) the presence of BCP between the proton (H) and acceptor (Y) is a confirmation of the existence of hydrogen bonding interaction, (ii) the value of the charge density ρ_{BCP} should be within the range 0.0020–0.0400 a.u. and (iii) the corresponding Laplacian $\nabla^2\rho_{BCP}$ at BCP should be within the range 0.0240–0.1390 a.u. In addition, the electron density value calculated at the BCPs of the intermolecular hydrogen bonds may be treated as a measure of the hydrogen bond strength. A trend of increasing ρ_{BCP} and $\nabla^2\rho_{BCP}$ at hydrogen bond critical points with increasing hydrogen bond strength was first noted by Carroll and Bader [40] and it was later confirmed by other authors [41,42].

The AIM theory is applied here to analyze the characteristics of the intermolecular hydrogen bond critical points appeared in the acetamide species. The topological parameters – electron density (ρ_{BCP}), Laplacian of electron density ($\nabla^2\rho_{BCP}$); energetic parameters – kinetic electron energy density (G_{BCP}), potential electron energy density (V_{BCP}) and total electron energy density (H_{BCP}) at BCP for each intermolecular hydrogen bonds appeared in the acetamide dimer, trimer and tetramers are given in Tables 5 and 6.

Table 5: AIM topological analysis of the hydrogen bonds in the dimer and trimer species of acetamide calculated at B3LYP/6-311++G** level of theory.

Parameter[a]	Dimer		Trimer		
	H4···O11	H14···O2	H4···O11	H22···O2	H14···O20
ρ_{BCP}	0.0302	0.0302	0.0266	0.0267	0.0266
$\nabla^2\rho_{BCP}$	0.1024	0.1024	0.1064	0.1067	0.1065
$\lvert\lambda_1\rvert/\lambda_3$	0.2355	0.2355	0.2047	0.2049	0.2049
G_{BCP}	0.0245	0.0245	0.0297	0.0297	0.0297
H_{BCP}	0.0011	0.0011	0.0039	0.0039	0.0039
V_{BCP}	-0.0233	-0.0233	-0.0258	-0.0258	-0.0258
$E_{H\cdots O}$	-7.31	-7.31	-8.09	-8.09	-8.09
ε	0.0443	0.0443	0.0027	0.0027	0.0027

The AIM analysis clearly shows that almost all of the hydrogen bonds in the acetamide species have a low charge density, ρ in the range of 0.0075-0.0302 a.u., positive Laplacian $\nabla^2\rho$ ranging from 0.0261 to 0.1024 au and the ratio of the perpendicular contractions of ρ to its parallel expansion $\lvert\lambda_1\rvert/\lambda_3$ is <1. Accordingly, the calculated topological parameters meet the Koch and Popelier criteria [39]. Moreover, the charge density values are slightly

dependent on the involved geometrical distance; therefore, a higher density (0.0302 a.u.) is observed for the dimer at H4···O11 and H14···O2 BCPs because there is a lower hydrogen bond length (1.868 Å). The cyclic acetamide trimer has three equivalent hydrogen bonds H4···O11, H22···O22 and H14···O20 with a charge density value is 0.0266 a.u., which is lower than that obtained in the dimer and is in accordance with the lengthening of the hydrogen bonds observed in the trimer. In the tetramers the charge densities calculated at H4···O11 and H14···O2 BCPs are relatively lower than that found in the dimer, which may be explained the charge redistribution upon formation of tetramers. The lowest charge density (0.0075 a.u.) is found at H36···O2 and H25···O11 BCPs appeared in the C33-H36···O2 and C24-H25···O11 hydrogen bonds in tetramer 1. These later are classified as the weakest hydrogen bond in the complex. The AIM analyses are in agreement with the geometrical parameters. In the tetramer 2, the charge densities calculated at H4···O11, H14···O2, H31···O2, H13···O29, H22···O11 and H5···O20 BCPs are in the range 0.0201-0.0278 a.u.

The average charge densities calculated at hydrogen bond critical points are 0.0191 and 0.0228 a.u. in the tetramer 1 and tetramer 2, respectively. This result clearly shows the high stability of the tetramer 2 in comparison to the tetramer 1. According to the electron density values at BCP, the strength of various intermolecular hydrogen bonding interactions are in the following order as: H4···O11 ≈ H14···O2 (dimer) > H4···O11 ≈ H14···O2 (tetramer 1) > H4···O11 ≈ H14···O2 (tetramer 2) > H4···O11 ≈ H22···O2 ≈ H14···O20 (Trimer) > H5···O20 ≈ H13···O29 (tetramer 1) > H31···O2 ≈ H22···O11 > H5···O20 ≈ H13···O29 (tetramer 2) > H25···O11 ≈ H36···O2 (tetramer 1). The order of hydrogen bond strength in the acetamide species is well consistent with the stabilization energies obtained by the NBO analysis. In addition, for all hydrogen bonds, the quantities $|\lambda_1|/\lambda_3$ are found to be less than 1. On the basis of the quantity of $|\lambda_1|/\lambda_3$, the strongest hydrogen bonds are observed for the acetamide dimer (0.2355), while the weakest hydrogen bonds are H25···O11 and H36···O2 (0.1714) formed in the tetramer 1. According to Rozas et al. [43], weak hydrogen bonds are characterized by $\nabla^2\rho_{BCP} > 0$ and $H_{BCP} > 0$ and they are mainly electrostatic in nature.

Table 6: AIM topological analysis of the hydrogen bonds in the tetramers species of acetamide calculated at B3LYP/6-311++G** level of theory.

	Parameter[a]	H4···O11	H14···O2	H5···O20	H13···O29	H25···O11	H36···O2
Tetramer 1	ρ_{BCP}	0.0282	0.0282	0.0216	0.0216	0.0075	0.0075
	$\nabla^2\rho_{BCP}$	0.0940	0.0940	0.0800	0.0800	0.0261	0.0260
	$\lvert\lambda_1\rvert/\lambda_3$	0.2341	0.2341	0.2089	0.2089	0.1714	0.1714
	G_{BCP}	0.0222	0.0222	0.0176	0.0176	0.0055	0.0055
	H_{BCP}	0.0013	0.0013	0.0024	0.0024	0.0010	0.0010
	V_{BCP}	-0.0210	-0.0210	-0.0151	-0.0151	-0.0045	-0.0045
	$E_{H\cdots O}$[b]	-6.58	-6.58	-4.73	-4.73	-1.41	-1.41
	ε	0.0519	0.0519	0.0522	0.0522	0.0635	0.0635
	Parameter[a]	H4···O11	H14···O2	H31···O2	H22···O11	H5···O20	H13···O29
Tetramer 2	ρ_{BCP}	0.0278	0.0278	0.0205	0.0205	0.0201	0.0201
	$\nabla^2\rho_{BCP}$	0.0924	0.0924	0.0866	0.0866	0.0768	0.0768
	$\lvert\lambda_1\rvert/\lambda_3$	0.2329	0.2329	0.1864	0.1864	0.1934	0.1936
	G_{BCP}	0.0218	0.0218	0.0184	0.0184	0.0166	0.0166
	H_{BCP}	0.0012	0.0012	0.0033	0.0033	0.0026	0.0026
	V_{BCP}	-0.0206	-0.0206	-0.0151	-0.0151	-0.0140	-0.0140
	$E_{H\cdots O}$[b]	-6.46	-6.46	-4.74	-4.74	-4.39	-4.39
	ε	0.0505	0.0505	0.0118	0.0118	0.0083	0.0083

[a] The quantities are in atomics units. [b] Hydrogen bond energies are in kcal/mol.

On the basis of these parameters all hydrogen bonds formed the acetamide species are weak. According to Espinosa [44] the hydrogen bond energy (E_{HB}) and potential energy density (V_{BCP}) at H···O contact is E_{HB} = (½)

V_{BCP}. The binding energies of the dimer, trimer, tetramer 1 and tetramer 2 are the sum of the energies of all intermolecular interactions and these are calculated as −61.19, −100.95, −106.38 and −113.65 kJ/mol, respectively. Another important parameter is the ellipticity (ε) defined as $(\lambda_1/\lambda_2) - 1$. The ellipticity measures the extent to which charge is preferentially accumulated. In terms of the orbital model of electronic structure, the ellipticity provides a quantitative measure of the π-bond character and of the delocalization electronic charge. Also, ellipticity is a measure of bond stability; high ellipticity values indicate instability of the bond [45–47]. The ellipticity values calculated for all hydrogen bonds in the acetamide species are given in Tables 5 and 6. The order of instability of hydrogen bond in the acetamide species is: H25···O11 and H36···O2 (tetramer 1) > H5···O20 and H13···O29 (tetramer 1) > H4···O11 ≈ H14···O2 (tetramer 1) > H4···O11 and H14···O2 (tetramer 1) > H4···O11 and H14···O2 (dimer) > H4···O11 and H14···O2 (tetramer 2) > H4···O11 and H14···O2 (dimer) > H31···O2 and H22···O11 (tetramer 2) > H4···O11 ,H22···O2 and H14···O20 (Trimer). The average ellipticity is much larger for hydrogen bonds in tetramer 1 (0.1117) than for hydrogen bonds in tetramer 2 (0.0235). Therefore, the hydrogen bonds in tetramer 2 are more stable than of hydrogen bonds in tetramer 1.

4.3. Vibrational analysis

Vibrational spectroscopy is one of the most useful experimental tools to study the hydrogen bonded clusters. The vibrational analysis of the acetamide monomer, dimer, trimer and tetramers are performed taking into account the experimental IR spectrum of acetamide in the solid phase. The calculated vibrational wavenumbers are higher than their experimental values for the majority of the normal modes. Two factors may be responsible for the discrepancies between the experimental and computed wavenumbers. The first is caused by the environment (gas and solid phase) and the second is due to the fact that the experimental values are an anharmonic wavenumbers while the calculated values are harmonic ones. The comparison of the predicted infrared and Raman spectra for the different acetamide species with the corresponding experimental ones can be seen in Figures 2 and 3.

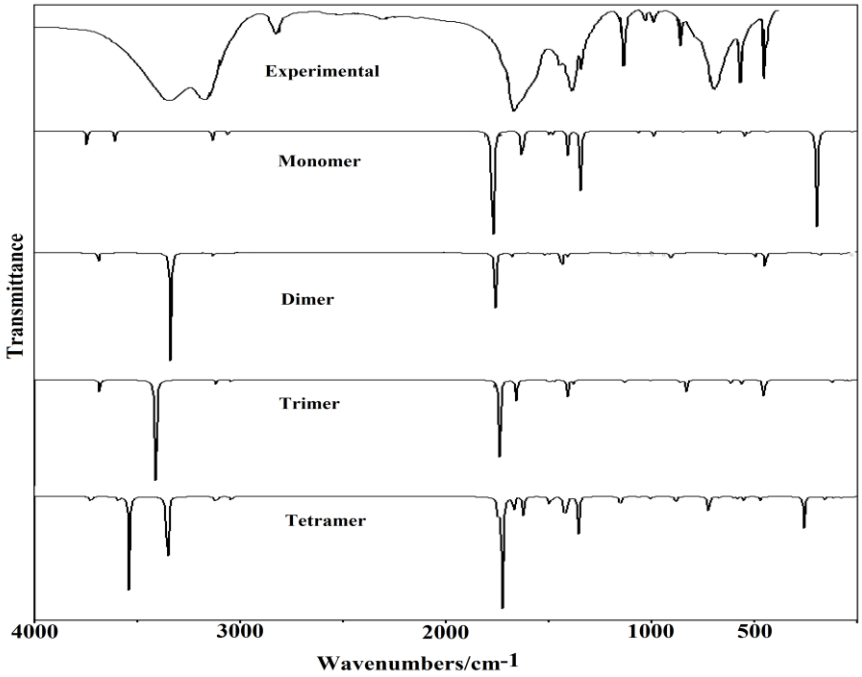

Figure 2: Comparison between experimental infrared spectrum of acetamide and infrared spectra of monomer, dimer, trimer and average tetramer form calculated by using B3LYP/6-311++G** level.

The experimental and calculated SQM wavenumbers of monomer, dimer, trimer, tetramer 1 and tetramer 2 using the B3LYP/6-311++G** method and the complete assignment of the observed bands are shown in Table 7. The molecule under consideration belongs to the primary amide family group. In the infrared spectra of the primary amide, one can observe two bands at 3350 and 3180 cm^{-1} which are assigned to the NH stretching asymmetric and symmetric vibrations, respectively.

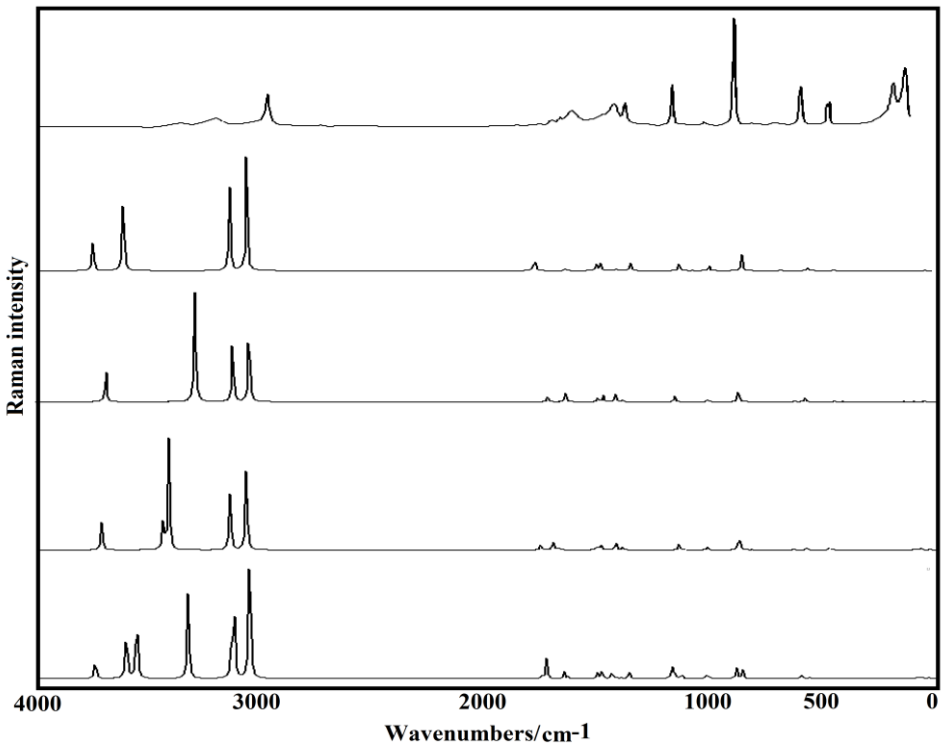

Figure 3: Comparison between experimental Raman spectrum of acetamide and Raman spectra of monomer, dimer, trimer and average tetramer form calculated by using B3LYP/6-311++G** level.

In addition, the band observed near 1650 cm^{-1} arises mainly from the C=O stretching vibration with minor contributions from the out-of-phase C–N stretching vibration, the C–C–N deformation and the N–H in-plane bend. In dilute, non-polar solvents, i.e. in the absence of hydrogen bonding, the N-H stretching bands occur at about 3500 cm^{-1} and 3400 cm^{-1}. In the solid state and in the presence of hydrogen bonding, these bands are shifted by about 150 cm^{-1} to about 3350 cm^{-1} and 3200 cm^{-1}. Both primary and secondary amides may exhibit a number of bands due to different hydrogen-bond states, e.g. dimers, trimers, tetramers, etc. The bands are concentration and solvent-dependent. The amide band due to the C=O stretching vibration is often referred as the primary amide band. Primary amides have a very strong band due to the C=O stretching vibration at 1670-1650 cm^{-1} in the solid phase, the band appearing at 1690-1670 cm^{-1} for a dilute solution using a non-polar solvent. The carbonyl absorption band is obviously greatly influenced by solvents, with which hydrogen bonds may be formed. In the case of clusters where hydrogen bonding interaction is manifested, the N-H stretching frequency shifts to a lower value and its intensity increases. The effect of hydrogen bonding on the vibration of linear acetamide cluster has been reported by Esrafili et al. [14]. They showed that the N-H stretching frequency decreases when the acetamide chain becomes longer. The change of the N-H stretching vibration upon the formation of the acetamide clusters has also been discussed by Mahadevi et al. [14]. They have showed a red shift of the N-H stretching vibration as the cluster size increases from 1 to 15. For the acetamide molecule, the very strong bands observed at 3347 and 3178 cm^{-1} in the FT-IR spectrum and the weak bands observed at 3591 and 3324 cm^{-1} in the Raman spectrum are assigned to NH_2 asymmetric and symmetric stretching vibrations respectively. The asymmetric and symmetric NH_2 stretching vibrations are calculated for the acetamide monomer at 3573 and 3443 cm^{-1}, respectively. The very strong band appeared at 1674 cm^{-1} corresponds to the C=O stretching vibration. This stretching vibration is calculated at 1696 cm^{-1}. Upon dimerization, the NH_2 and C=O stretching vibrations are redshifted by 423 and 45 cm^{-1}, respectively. In the trimer structure, the NH_2 and C=O stretching vibrations are redshifted by 326 and 74 cm^{-1}. Moreover, in comparison to the monomer, the tetramer 1 exhibits a notable redshifts of the NH_2 and C=O stretching vibrations with 396 and 77 cm^{-1}, while the tetramer 2 these vibrations are downshifted by 364 and 87 cm^{-1}, respectively. The shifts of NH_2 and C=O stretching modes

to lower wavenumber region are due to the intermolecular hydrogen bonding formed in the acetamide species. In primary amides, C–N stretching vibration appears in the region 1430–1390 cm^{-1} [48]. The C–N stretching mode is usually coupled with C–C–O deformation and makes significant contribution to the Raman band at 1260 cm^{-1}. The IR counterpart is observed at the same wavenumber. The C–C–N bending mode is observed in Raman at 274 cm^{-1}. For the acetamide, the medium bands observed at 1352 cm^{-1} and 1359 cm^{-1} in FT-IR spectrum and Raman spectra, respectively, are may be due to the C-N stretching vibrations. These vibrations are calculated in the range 1390-1354 cm^{-1} in the acetamide tetramers. In order to reproduce the infrared spectrum of the acetamide, we have given in Figure 4 the comparison between the experimental infrared spectrum of acetamide in solid phase with the average theoretical unscaled wavenumbers in gas phase for the monomer, dimer, trimer, tetramer 1 and tetramer 2 at B3LYP/6-311++G**. As shown in Figure 4, the overage spectrum reproduces well the experimental one.

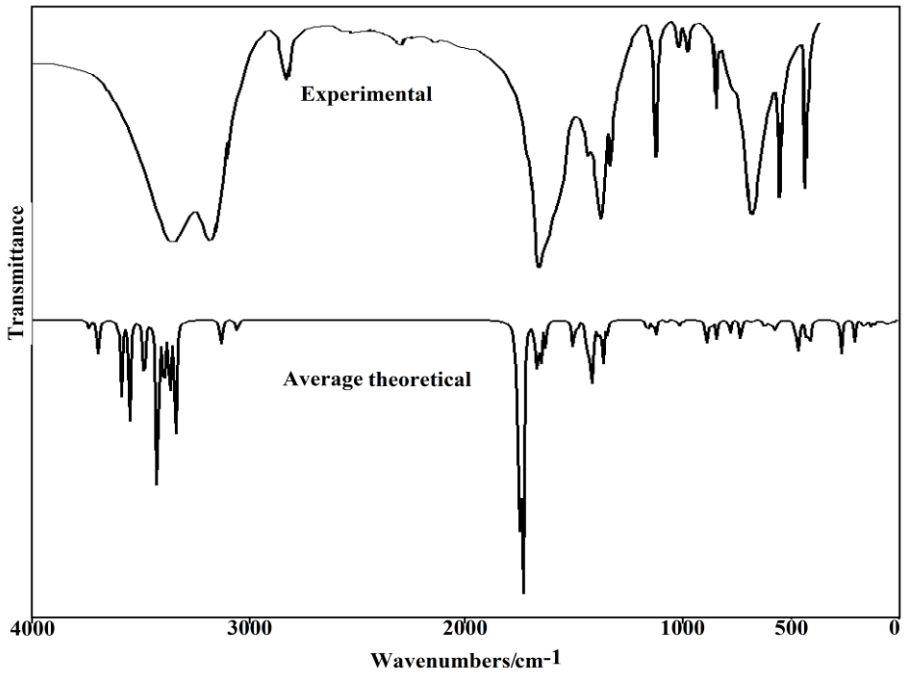

Figure 4. Comparison between the experimental infrared spectrum of acetamide in solid phase (upper) with the average theoretical unscaled in gas phase for the monomer, dimer, trimer, tetramer 1 and tetramer 2 at B3LYP/6-311++G** (bottom).

Table 7: Observed and calculated wavenumbers (cm^{-1}) and assignment for all the studied species of acetamide.

Experimental		Monomer		Dimer		Trimer		Tetramer 1		Tetramer 2	
IR[a]	Raman[a]	SQM[c]	Assignment[a]	SQM[c]	Assignment[a]	SQM[c]	Assignment[a]	SQM[c]	Assignment[a]	SQM[c]	Assignment[a]
	3591 vw	3573	ν_aNH_2	3530	ν_aNH_{2op}	3531	νNH	3572	νaNH_2op	3537	νaNH_2
3347 s	3324 w			3530	ν_aNH_{2ip}	3531	νNH	3572	νaNH_2ip	3537	νsNH_2
		3443	ν_sNH_2			3531	νNH	3443	νsNH_2op	3432	νsNH_2
						3271	νNH	3443	νsNH_2ip	3428	νaNH_2
						3271	νNH	3398	νaNH	3330	νaNH_2
	3219 sh					3247	νNH	3395	νsNH	3326	νsNH_2
								3217	νsNH	3243	νaNH_2
3178 s	3164 w			3191	ν_sNH_{2op}			3177	νaNH	3209	νsNH_2
3146 sh	3132 sh			3150	ν_sNH_{2ip}			2995	$\nu_aCH_3(15)$	2998	ν_aCH_3 ip
3096 sh	3011 sh							2995	$\nu_aCH_3(6)$	2998	$\nu_aCH_3$op
3049 sh	2970 sh	2990	ν_aCH_3	2990	$\nu_aCH_3(6)$	2991	$\nu_aCH_3(24)$	2991	$\nu_aCH_3(24)$	2989	ν_aCH_3 ip

		2990	ν_aCH_3	2990	ν_aCH_3(15)	2990	ν_aCH_3(6)	2991	ν_aCH_3(33)	2989	$\nu_aCH_3$ip
						2989	ν_aCH_3(15)	2983	ν_aCH_3(24)	2987	ν_aCH_3 ip
				2987	ν_aCH_3(6)	2986	ν_aCH_3(6)	2983	ν_aCH_3(33)	2987	$\nu_aCH_3$ip
				2987	ν_aCH_3(15)	2986	ν_aCH_3(15)	2981	ν_aCH_3(6)	2983	$\nu_sCH_3$ip
						2985	ν_aCH_3(24)	2981	ν_aCH_3(15)	2982	$\nu_aCH_3$ip
	2936 m	2919	ν_sCH_3	2919	ν_sCH_3(15)	2918	ν_sCH_3(15)	2918	ν_sCH_3(6)	2920	$\nu_sCH_3$op
	2911 sh			2919	ν_sCH_3(6)	2918	ν_sCH_3(24)	2918	ν_sCH_3(15)	2920	$\nu_sCH_3$ip
2827 w	2853 vw					2918	ν_sCH_3(6)	2916	ν_sCH_3(24)	2918	ν_sCH_3
	2700 vw							2915	ν_sCH_3(33)	2918	$\nu_sCH_3$ip
	1738 vw							1727	νC28=O29	1725	νsC=O
1722 sh								1725	νC19=O20	1725	νaC=O
1713 sh	1697 sh							1713	νC10=O11	1702	νaC=O
1674 vs	1681 w	1696	νC1=O2	1673	νaC=O	1670	νaC=O			1653	δNH_2(N3)
	1658 sh			1651	νsC=O	1669	νaC=O	1670	δNH_2(N12)	1609	νsC=O
1642 sh	1648 w					1622	νsC=O	1620	δNH_2(N3)	1604	δNH_2(N12)
1613 sh	1592 m					1592	δNH_2(N3)	1619	νC1=O2	1593	δNH_2(N21)
1589 sh				1583	δNH_2(N12)	1586	δNH_2(N12)	1559	δNH_2(N30)	1588	δNH_2(N30)
1564 sh	1562 sh	1549	δNH_2	1571	δNH_2(N3)	1585	δNH_2(N21)	1559	δNH_2(N21) νC19-N21		
1472 sh								1483	δ_aCH_3(24)# δ_aCH_3(33)#	1463	νC10-N12
1456 w	1455 sh			1434	δ_aCH_3(6)	1433	δ_sCH_3(15)	1454	δ_aCH_3(33)	1454	νaC-C
				1431	δ_aCH_3(15)	1431	δ_aCH_3(24)	1449	δ_aCH_3(6)# δ_aCH_3(15)#	1436	δ_aCH_3(24)
						1431	δ_aCH_3(6)	1446	δ_aCH_3(24)	1436	δ_aCH_3(33)
1422 sh		1428	δ_aCH_3					1422	δ_aCH_3(24)	1414	δ_aCH_3(15)
						1411	δ_aCH_3(24)	1421	δ_aCH_3(33)	1414	δ_aCH_3(6)
	1410 m			1410	δ_aCH_3(15)	1411	δ_aCH_3(6)	1413	δ_aCH_3(6)	1411	δ_aCH_3(33)
		1410	δ_aCH_3	1410	δ_aCH_3(6)	1411	δ_aCH_3(15)	1413	δ_aCH_3(15)	1410	δ_aCH_3(24)
1400 s	1393 sh							1390	ρC10=O11 δ_aCH_3(15) νC10-N12	1396	δ_aCH_3(15) δ_aCH_3(6)
								1390	δ_aCH_3(6) νC1-N3	1390	νC1-N3
1352 m	1359 m			1364	νsC-N	1356	νC19-N21	1354	δ_sCH_3(24) νC28-N30#	1361	νC28-N30
1341 sh	1341 sh	1338	δ_sCH_3	1358	νaC-N	1352	νC10-N12	1351	δ_sCH_3(33)	1360	νC19-N21
1335 sh				1328	δ_sCH_3(6)	1352	δ_sCH_3(24)	1330	δ_sCH_3(6)	1333	δ_sCH_3(15)
	1319 sh			1325	δ_sCH_3(15)	1325	δ_sCH_3(6)	1330	δ_sCH_3(15)	1332	δ_sCH_3(6)
						1322	νC1-N3	1328	ρNH_2(N21)#	1325	δ_sCH_3(33)
1160 sh	1183 sh	1291	νC1-N3			1322	δ_sCH_3(15)	1326	ρNH_2(N30)#	1324	δ_sCH_3(24)
1143 m	1152 s			1119	ρNH_2(N12)			1124	ρNH_2(N3)		
				1114	ρNH_2(N3)			1119	ρNH_2(N12)	1095	ρNH_2(N21)
	1109 sh					1083	ρNH_2(N3)	1093	ρCH_3(24)	1094	ρNH_2(N30)
						1083	ρNH_2(N12)	1092	ρCH_3(33)	1086	ρNH_2(N3)
		1078	ρNH_2			1081	ρNH_2(N21)			1079	ρNH_2(N12)
1043 w								1037	ρCH_3(6)	1038	ρCH_3(15)

									$\rho CH_3(15)$		
						1035	$\rho CH_3(15)$	1037	$\rho CH_3(33)$	1038	$\rho CH_3(6)$
				1034	$\rho CH_3(15)$	1034	$\rho CH_3(24)$	1036	$\rho CH_3(24)^{\#}$ $\rho CH_3(33)^{\#}$	1033	$\rho CH_3(33)$ γC28=O29
		1030	ρCH_3	1034	$\rho CH_3(6)$	1034	$\rho CH_3(6)$	1030	$\rho CH_3(24)$	1033	$\rho CH_3(24)$ γC19=O20
1000 w	1013 w							996	$\rho CH_3(24)^{\#}$ $\rho CH_3(33)^{\#}$	985	$\rho CH_3(15)$
				979	$\rho CH_3(15)$	975	$\rho CH_3(6)$	991	$\rho CH_3(6)$ $\rho CH_3(15)$	983	$\rho CH_3(6)$
				978	$\rho CH_3(6)$	975	$\rho CH_3(15)$	987	$\rho CH_3(24)$	977	$\rho CH_3(24)$
		953	ρCH_3			974	$\rho CH_3(24)$	981	$\rho CH_3(24)$	977	$\rho CH_3(33)$
880 sh	881 vs							886	$\gamma NH_2(N3)^{\#}$ $\gamma NH_2(N12)^{\#}$	876	νsC-C
867 w								875	νC1-C6 νC10-C15	873	νaC-C
				840	νaC-C	829	νsC-C	846	νC19-C24	846	νC19-C24
	820 sh			837	νsC-C	823	νaC-C	842	νC28-C33	843	νC28-C33
781 sh	802 w	807	C1-C6	798	τNH_2ip	822	νaC-C	824	$\gamma NH_2(N3)^{\#}$ $\gamma NH_2(N12)^{\#}$	776	$\tau wNH_2(N12)$ $\gamma NH_2(N3)$
	766 sh			753	τwO---H	759	$\tau wNH_2(N12)$	754	$\tau wNH_2(N3)$ $\tau wNH_2(N12)$		
						736	$\tau wNH_2(21)$			735	$\gamma NH_2(N3)$
						735	$\tau wNH_2(N3)$			697	τC1-O2
707 s	700 w							670	τC1-N3 τC10-N12	690	τC19-O24 τC10-O11
								658	τC28-O29	652	$\gamma NH_2(N12)$
	611 sh	632	γC1=O2	602	γaC=O	603	γC19=O20	628	γC28=O29	651	τC10-O11
						602	γC10=O11	626	γC19=O20		
591 sh	596 sh			592	γsC=O	600	γC1=O2	596	γC1=O2$^{\#}$ γC10=O11$^{\#}$	592	ρC10=O11
583 s				574	ρC=Oop			584	ρC1=O2	584	τC19-O24 τC1-O2
574 sh	578 s									583	τC10-O11
569 sh	568 sh			568	ρC=Oip	553	ρaC=O	562	γC1=O23$^{\#}$ γC10=O11$^{\#}$	570	ρC1=O2
						552	ρaC=O	561	τC19-O20	557	ρC28=O29
						545	ρsC=O	546	ρC19=O20	555	γC1=O2
								537	ρC28=O29 $\tau wNH_2(N21)^{\#}$	552	γC10=O11
471 m	482 sh	539	ρC1=O2					491	τC19-O24	551	ρC19=O20
462 sh	461 w	486	τNH_2					491	$\tau wNH_2(N30)^{\#}$	460	δN12C10C15
458 sh				460	δaN-C-C	444	δN3C1C6	467	N12C10C15$^{\#}$ δN3C1C6$^{\#}$	452	δN30C28C33
442 sh	449 sh					444	δN12C10C15	448	δN12C10C15 δN3C1C6	449	δN21C19C24
		428	δN-C-C	439	δsN-C-C	433	δN21C19C24	444	δN21C19C24	442	δN3C1C6

						426	γNH_2(N3)	437	δN30C28C33		
				389	γNH_2(N3)	420	γNH_2(N21)			360	τC19-O24 τC10-O11
				385	τNH_2op	419	γNH_2(N12)	230	γNH_2(N21)	360	γNH_2(N21) γNH_2(N30) τwNH_2(N21) τwNH_2(N30)
	300 sh							229	γNH_2(N30)		
	211 sh	190	γNH_2					166	νO11---H4 νO20---H5[#]	174	δC10O11H22
	178 s							165	νO2---H36[#] νO11---H25[#]		
	142 sh			145	νaO---H					147	νaO---H
				141	νsO---H			134	νO2---H14 νO29---H13[#]	135	νsO---H
	124 s			129	γO---H	130	νsO---H	131	τC10-O11		
						117	νaO---H	127	τwCH_3(C24) [#] τwCH_3(C33) [#]		
	115 sh					116	νaO---H	119	νO20---H5 τwCH_3(C6)[#]	119	νO29---H13
						107	δC10O11H4			100	δC28O29H13
								99	δC1O2H36 τwCH_3(C15)[#]	99	τC-C
								94	δC10O11H25	93	νO11---H22 νO2---H31
										92	τC-N
								85	τwCH_3(C24)	84	νO20---H5
				83	γNH_2(N12)	78	τC1-N3			75	τC19-O24 τC1-O2
						78	τC10-N12	69	τwCH_3(C6)[#]	73	τwCH_3(C6)
				74	τwO---Hip	74	τC19-N21	65	τC10-O11	65	τC19-O24
						56	δC19O20H14	62	δC28O29H13	64	τC1-O2
						55	δC1O2H22	60	δC19O20H5	54	τC19-O24 τC1-N3
						53	τwCH_3(C15)	50	τC28-C33	50	δC1O2H31
				48	τCH_3op	50	τwCH_3(C6)	50	τwCH_3(C33)	41	τC1-O2
				37	τwO---Hop	42	τwCH_3(C24)	49	δC28O29H13	35	τC19-O24
				32	τCH_3ip	31	τC1-O2	31	δC19O20H5	34	δC19O20H5
		23	τCH_3					22	τC1-N3	30	τC-N τwCH_3(C15) τwCH_3(C33)
								22	δC1O2H36	25	τ N3-H5
						17	τC19-O20	18	δC10O11H25		
						15	τC10-O11	17	τC1-O2		
								13	τwCH_3(C24)	11	τC-C

Abbreviations: ν, stretching; γ, deformation out of plane; wag, wagging; τ , torsion; ρ, rocking; twis, twisting; δ, deformation; a, antisymmetric; s, symmetric; ip, in-phase; op, out-of-phase. [a]This work; [b]DFT B3LYP/6-31G*; [c]From scaled quantum mechanics force field; [d]Units are km.mol^{-1}; [e]Raman activities in Å^4 (amu)$^{-1}$;[#]Assigned by *GaussView* program [25].

Conclusion

In this work, molecular structures of the acetamide and its hydrogen bonded dimer, trimer and tetramers have been optimized using the hybrid B3LYP method with 6-311++G** basis set. The optimized geometry of tetramer 2 reproduces well the experimental structure of the acetamide. The stability of the acetamide structures was investigated using NBO and AIM analysis. The NBO analysis reveals that the total energy contribution is mainly due to the interaction between lone pairs of the oxygen atoms and σ*(N-H) antibonding orbitals, $\Delta ET_{LP\rightarrow\sigma^*}$, which clearly show that the highest stability is found in tetramer 2. In addition, the AIM analysis confirmed that all the hydrogen bonds in the acetamide species are weak and the tetramer 2 may be more stable than the tetramer 1. The natural population analysis showed that hydrogen bonds in tetramer 2 cause a significant electrostatic interaction in comparison to tetramer 1. The vibrational analysis of acetamide monomer, dimer, trimer and tetramers has been carried out based on SQM force field obtained by B3LYP density functional theory calculations. The redshifts of the N-H and C=O stretching vibrations are due to the formation of intermolecular hydrogen bonding. The results of the vibrational analysis reveals that the tetramer species reproduce better the infrared spectra of acetamide.

References

1. Jeffrey G.A., Saenger W., *Hydrogen Bonding in Biological Structures* (Springer-Verlag, New York, 1991).
2. A.V. Finkelstein and O.B. Ptitsyn, *Protein Physics* (Academic Press, London, 2002).
3. Gu Z., Ridenour C.F., Bronniamann C.E., Iwashita T., McDermott A., *J. Am. Chem. Soc.* 118 (1996) 822.
4. Kumar G.A., McAllister M.A., *J. Org. Chem.* 63 (1998) 6968.
5. Cieplak P., Kollman P.A., *J. Comput. Chem.* 12 (1991) 1232.
6. Strohmeier M., Stueber D., Grant D.M., *J. Phys. Chem.* A107 (2003) 7629.
7. Lipsitz R.S., Sharma Y., Brooks B.R., Tjandra N., *J. Am. Chem. Soc.* 124 (2002) 10621.
8. Lutz H.D., *J. Mol. Struct.* 646 (2003) 227.
9. Scheiner S., Kar T., Pattanayak J., *J. Am. Chem. Soc.* 124 (2002) 13257.
10. Görbitz C.H., *Curr. Opin. Solid State Mater. Sci.* 6 (2002) 109.
11. Görbitz C.H., *J. Mol. Struct. Theochem,* 775 (2006) 9.
12. Behzadi H., Hadipour N.L., Mirzaei M., *Biophys. Chem.* 125 (2007) 179.
13. Samadi Z., Mirzaei M., Hadipour N.L., Khorami S.A., *J. Mol. Graph. Model.* 26 (2008) 977.
14. Esrafili M. D., Behzadi H., Hadipour N.L., *Theor. Chem. Account*. 121 (2008) 135.
15. Mahadevi A.S., Neela Y.I., Sastry G.N., *Phys. Chem. Chem. Phys.* 13 (2011) 15211.
16. Beg H., De S.P., Ash S., Das D., Misra A., *Comput. Theo. Chem.* 1005 (2013) 1.
17. Abdelmoulahi H., Bahri H., Bahri M., Nasr S., *J. Mol. Liq.* 197 (2014) 251.
18. Reed A.E., Curtis L.A., Weinhold F., *Chem. Rev.* 88(6) (1988) 899.
19. Glendening E.D., Badenhoop J.K., Reed A.D., Carpenter J.E., Weinhold F., *NBO 3.1* (University of Wisconsin, Madison, 1996).
20. Ghalla H., Govindarajan M., Flakus H.T., Issaoui N., Yaghmour S.J., Oujia B., *Spectrochim. Acta Part A* 136 (2015) 579.
21. Ghalla H., Issaoui N., Govindarajan M., Flakus H.T., Jamroz M.H., Oujia B., *J. Mol. Struct.* 1059 (2014) 132.
22. Bader R.F.W., *Atoms in Molecules, A Quantum Theory* (Oxford University Press, Oxford, 1990).
23. Biegler-Köning F., Schönbohm J., Bayles D., *J. Comput. Chem.* 22 (2001) 545.
24. Pulay P., Fogarasi G., Pongor G., Boggs J.E., Vargha A., *J. Am. Chem. Soc.* 105 (1983) 7037.
25. Nielsen A.B., Holder A.J., *Gauss View* 5.0, *User's Reference, GAUSSIAN Inc.*, (Pittsburgh, PA, 2009).
26. Bats J.W., Haberecht M.C., Wagner M., *Acta. Cryst.* E59 (2003) o1483.
27. Frisch M.J. et al., *Gaussian 09, Revision A.02, Gaussian, Inc* (Pittsburgh, PA, 2009).
28. Boys S.F., Bernardi F., *Mol. Phys.* 19 (1970) 553.
29. Biegler-Köning F., Schönbohm J., Bayles D., *AIM2000; a program to analyze and visualize atoms in molecules, J. Comput. Chem.* 22 (2001) 545.

30. Brandán S.A., Eroğlu E., Ledesma A.E., Oltulu O., Yalçınkaya O.B.,. *J. Mol. Struct.* 993 (2011) 255.
31. Lizarraga E., Romano E., Rudyk R.A., Catalán C.A.N., Brandán S. A., *Spectrochim. Acta Part A* 97 (2012) 202.
32. Piro O.E., Echeverría G. A., Lizárraga E., Romano E., Catalán C.A.N., Brandán S.A., *Spectrochimica Acta Part A* 101 (2013) 196.
33. Bichara L.C. Brandán S.A., *J. Mol. Liq.* 181 (2013) 34.
34. Roldán M.L., Ledesma A.E., Raschi A.B., Castillo M.V., Romano E., Brandán S.A., *J. Mol. Struct.* 1041 (2013) 73.
35. Guzzetti K., Brizuela A.B., Romano E., Brandán S.A., *J. Mol. Struct.* 1045 (2013) 171.
36. Ghalla H., Issaoui N., Castillo M.V., Brandán S.A., Flakus H.T., *Spectrochim. Acta A*, 121 (2014) 623.
37. Sundius T., *J. Mol. Struct.* 218 (1990) 321.
38. Foster J.P., Weinhold F., *J. Am. Chem. Soc.* 102 (1980) 7211.
39. Koch U., Popelier P., *J. Phys. Chem.* A 99 (1995) 9747.
40. Carroll M.T., Bader R.F.W., *Mol. Phys.* 63 (1988) 387.
41. Platts J.A., Howard S.T., Bracke B.R.F., *J. Am. Chem. Soc.* 118 (1996) 2726.
42. Luis Perez-Lustres J., Br€auer M., Mosquera M., Clark T., *Phys. Chem. Chem. Phys.* 3 (2001) 3569.
43. Rozas I., Alkorta I., Elguero J., *J. Am. Chem. Soc.* 122 (2000) 11154.
44. Espinosa E., Molins E., Lecomte C., *Chem. Phys. Lett.* 285 (1998) 170.
45. Bader R.F.W., *Atoms In Molecules-A Quantum Theory* (Oxford University Press, New York, 1990).
46. Popelier P.L.A., *Atoms In Molecules-An Introduction* (Pearson Education, Harlow, 2000).
47. Bader R.F.W., *Chem. Rev.* 91 (1991) 893.
48. Dollish F.R., Fateley W.G., Bentley F.F., *Characteristic Raman Frequencies of Organic Compounds* (Wiley, New York, 1974).